

## Accelerating Rare Reactive Events by Means of a Finite Electronic Temperature

Joost VandeVondele and Ursula Rothlisberger\*

Contribution from the Laboratory of Inorganic Chemistry, ETH Zurich, 8093 Switzerland

Received December 7, 2001. Revised Manuscript Received February 8, 2002

**Abstract:** The range of chemical problems that are directly accessible to first-principles molecular dynamics simulations based on density functional theory is extended with a novel method apt to accelerate rare reactive events. The introduction of a finite electronic temperature within the Mermin formalism leads to a lowering of chemical activation barriers and thus to an exponential enhancement of the rate at which these reactions are observed during a first-principles molecular dynamics simulation. The method presented here makes direct use of the intrinsic chemical information encoded in the electronic structure, and is therefore able to lower selectively chemically relevant activation energies even in systems where many competing low-energy pathways for conformational transitions or diffusive motions are present. The performance of this new approach is demonstrated for a series of prototypical chemical reactions in gas and in condensed phase. A typical acceleration that can be achieved is, for example, a factor of  $10^5$  for the cis–trans isomerization of peroxynitrous acid in aqueous solution at room temperature.

### I. Introduction

Electronic structure calculations have become an important tool for a detailed understanding of chemical reaction mechanisms. A particular versatile approach in this respect is the recently developed first-principles molecular dynamics (Car–Parrinello) method.<sup>1,2</sup> This technique allows for the evaluation of finite temperature properties and thus for the in situ study of chemical reactions in gas phase and in solution<sup>3</sup> within the framework of density functional theory (DFT)<sup>4,5</sup> or other quantum chemical electronic structure methods.<sup>6</sup> First-principles molecular dynamics simulations are especially valuable for complex reactive systems in which a reaction coordinate is not known a priori and may involve a nontrivial combination of multiple degrees of freedom. A few snapshots of the dynamics of such a system can often guide chemical intuition into previously unexpected directions. Indeed, for systems with relatively low activation barriers, chemical reactions can occur spontaneously during a molecular dynamics (MD) run, and hence reveal direct atomistic information about the reactive process. Unfortunately, due to the relatively high computational cost, only relatively short time periods, typically 1–100 ps, can currently be simulated. The observation of spontaneous reactions is thus only possible for fast processes with low activation barriers. Many orders of magnitude longer simulation times

would be needed to observe chemical reactions with activation barriers of the order of 10–30 kcal/mol. At present, slow reactions in complicated systems can only be studied efficiently if some information about the reaction pathways is known. In this case, the system can be constrained along an a priori chosen approximate reaction coordinate and be pulled over the activation barrier.<sup>7,8</sup> Because this information is not always available, and an inappropriately chosen reaction coordinate can yield misleading results, it is of primary importance to develop methods that are able to explore rare, reactive configurations for complex systems in an efficient and unprejudiced way.

One effective way to increase the number of rare events during a simulation is biased sampling.<sup>9–16</sup> In this approach, an additional (bias) potential that guides the system through the regions of interest is added to the original Hamiltonian. In this way, an enhanced sampling of activated events can, in principle, be achieved in a straightforward manner by choosing a bias potential that selectively lowers the activation energy. Because the rates for barrier crossing depend exponentially on the energy of the transition state, the required computer time for a statistically meaningful sampling of the system, and accordingly for a comprehensive understanding of its chemical reactivity, is orders of magnitude lower than in the original unbiased ensemble. Note that biased sampling yields exact

\* To whom correspondence should be addressed. E-mail: uro@inorg.chem.ethz.ch.

- (1) Car, R.; Parrinello, M. *Phys. Rev. Lett.* **1985**, *55*, 2471.
- (2) For a recent review of the Car–Parrinello method see, e.g.: Marx, D.; Hutter, J. In *Modern Methods and Algorithms of Quantum Chemistry*; Grotendorst, J., Ed.; NIC Series: Jülich, 2000; Vol. 1, p 301.
- (3) For a recent review of applications of the Car–Parrinello method see, e.g.: Rothlisberger, U. In *Computational Chemistry: Reviews of Current Trends*; Leszczynsky, J., Ed.; World Scientific: Singapore, 2001; Vol. 6, p 33.
- (4) Hohenberg, P.; Kohn, W. *Phys. Rev. B* **1964**, *136*, 864.
- (5) Kohn, W.; Sham, L. J. *Phys. Rev. A* **1965**, *140*, 1133.
- (6) See, e.g.: Hartke, B.; Carter, E. A. *J. Chem. Phys.* **1992**, *97*, 6569.

- (7) Carter, E. A.; Ciccotti, G.; Hynes, J. T.; Kapral, R. *Chem. Phys. Lett.* **1989**, *156*, 472.
- (8) Sprik, M.; Ciccotti, G. *J. Chem. Phys.* **1998**, *109*, 7737.
- (9) Torrie, G. M.; Valleau, J. P. *J. Chem. Phys.* **1977**, *66*, 1402.
- (10) Huber, T.; Torda, A. E.; van Gunsteren, W. F. *J. Comput. Chem.* **1994**, *8*, 695.
- (11) Grubmüller, H. *Phys. Rev. E* **1995**, *52*, 2893.
- (12) Voter, A. F. *J. Chem. Phys.* **1997**, *106*, 4665.
- (13) Voter, A. F. *Phys. Rev. Lett.* **1997**, *78*, 3908.
- (14) Steiner, M. M.; Genilloud, P.-A.; Wilkins, J. W. *Phys. Rev. B* **1998**, *57*, 10236.
- (15) Gong, X. G.; Wilkins, J. W. *Phys. Rev. B* **1999**, *59*, 54.
- (16) VandeVondele, J.; Rothlisberger, U. *J. Chem. Phys.* **2000**, *113*, 4863.

canonical averages, whereas the underlying dynamics is fictitious. Several approaches for the construction of such bias potentials have been suggested.<sup>9–16</sup> For reactions which proceed via a relatively simple geometric pathway or involve an energy barrier of known physicochemical origin, it is often possible to design an efficient bias potential.<sup>9,16</sup> If the reaction pathway is difficult to express in a geometrical way or involves many degrees of freedom that are not known beforehand, current methods typically use local properties of the potential energy surface, such as, for example, the Hessian and its derivatives, for the construction of an appropriate bias potential, and occasionally impressive gains in computational efficiency of up to 10 orders of magnitude can be achieved.<sup>13</sup> However, the information that is locally contained in the potential energy surface near a minimum configuration is not always representative for the properties of the reactive transition state and is thus not sufficient for the design of a successful bias potential to accelerate rare reactive events in many complex systems. In particular, the low frequency modes of the Hessian near the minimum often do not yield specific information about the possible chemical reactions of the system since these events can involve the breaking of bonds that are initially much stiffer than the typical soft modes such as, for example, torsional modes. Additionally, in realistic chemical systems, many low barriers exist related to solvent motion or to the overall rotation of ligands, that only lead to new conformers. The barrier for the actual reactive process lies at much higher energy and is therefore hard to locate. In general, methods that are only based on the local information of the potential energy surface have a low efficiency for the acceleration of rare reactive events since they cannot discriminate between events of high or low chemical relevance.

In this paper, we present a novel *ab initio* molecular dynamics method that makes direct use of the electronic structure of the reactive system to enhance the sampling of rare chemical events in complex systems. Comprehensive information about the intrinsic chemical reactivity of a system is contained in its electronic structure. This simple fact has been used by chemists for decades and lies at the roots of the overwhelming success of frontier orbital theory.<sup>17</sup> The intimate link between electronic structure and chemical properties has been emphasized within DFT with the concepts of reactivity indices such as, for example, chemical hardness, softness, and Fukui functions.<sup>18,19</sup> In particular, the electronic Fukui functions correspond, within a frozen orbital picture, to the highest occupied orbital(s) (HOMO(s)) and the lowest occupied orbital(s) (LUMO(s)). They determine the electron-donor and electron-acceptor properties of a reactive system, respectively, whereas a linear combination of HOMOs and LUMOs is relevant in the context of radical reactions.<sup>18,19</sup> High softness values indicate that fluctuations in the number of electrons can occur easily.<sup>18,20</sup> Increasing the softness will therefore enhance the reactivity toward orbital-driven reactions.<sup>18,21</sup> This insight can be employed in sampling methods that use the electronic structure to construct a bias

potential that is efficient in guiding the system to chemically relevant regions of phase space, that is, more reactive conformations, without having to resort to *a priori* assumptions about likely reaction pathways based on atomic coordinates.

The simple electronic bias potential we present here in the context of first-principles molecular dynamics simulations exploits the electronic structure in a straightforward way by simulating the system at an increased electronic temperature  $T^e$ . Through the introduction of a finite electronic temperature ( $T^e > 0$ ), electron density is transferred from the highest lying donor orbitals of the entire reactive system to its lowest lying acceptor orbitals, that is, its lowest-energy virtual states, thus enhancing its intrinsic reactivity. Indeed, the maximum hardness principle<sup>22–26</sup> implies that through the admixture of virtual excited states the system becomes softer,<sup>27</sup> that is, more reactive toward soft, orbital-driven reactions. We will show below that the difference between the finite temperature and the ground-state potential energy surface can be interpreted as a bias potential that guides the system toward regions with small electronic gaps. To examine the efficiency of this finite temperature-assisted acceleration (FTAA) approach in a quantitative manner for a variety of reactive systems, energy profiles along simple reaction coordinates have been calculated for a set of prototypical chemical reactions in gas and condensed phase, and the barrier heights at finite electronic temperature have been systematically compared with the 0 K results.

## II. Finite Electronic Temperature as a Chemical Driving Force

Here, we take  $H_2$  as an example of a simple two-state (HOMO–LUMO) dominated system which illustrates that the electronic gap near the transition state is often smaller than the one near the stable states. The bonding and antibonding molecular orbitals of this molecule, the HOMO and LUMO, are the chemically active orbitals. The reaction channels that are open to this system are homolytic or heterolytic breakage of the H–H bond, the former being the energetically favored reaction path in gas phase. With growing H–H distance, HOMO and LUMO become increasingly closer in energy until they reach complete degeneracy in the two equivalent free hydrogen radicals. The chemical bonding in the equilibrium geometry induces a lowering of the energy of the bonding orbital and, consequently, an increase of the energy of the antibonding orbital. The resulting large gap is reduced as soon as the bond is stretched, that is, as soon as the electronic configuration becomes less favorable. A similar lowering of the HOMO–LUMO gap at the transition state can be observed more generally also for other reactions<sup>28</sup> leading to a characteristic energy level diagram of the type shown in Figure 1. This effect can be rationalized by the qualitative argument that during a chemical reaction electron density is transferred from donor to acceptor states of the system, that is, as discussed above, within a frozen orbital picture, from the HOMO to the LUMO. This electronic redistribution induces a destabilization of the former

(17) Fukui, K.; Fujimoto, H. *Frontier Orbitals and Reaction Paths*; World Scientific: Singapore, 1997.

(18) See, e.g.: Chermette, H. *J. Comput. Chem.* **1999**, *20*, 129.

(19) Parr, R. G.; Yang, W. *Density-Functional Theory of Atoms and Molecules*; Oxford University Press: New York, 1989.

(20) Yang, W.; Parr, R. G. *Proc. Natl. Acad. Sci. U.S.A.* **1985**, *82*, 6723.

(21) Klopman, G. *Chemical Reactivity and Reaction Path*; Wiley: New York, 1974.

(22) Pearson, R. G. *J. Chem. Educ.* **1987**, *64*, 561.

(23) Pearson, R. G. *Acc. Chem. Res.* **1993**, *26*, 250.

(24) Parr, R. G.; Zhou, Z. *Acc. Chem. Res.* **1993**, *26*, 256.

(25) Chattaraj, P. K.; Lee, H.; Parr, R. G. *J. Am. Chem. Soc.* **1991**, *113*, 1855.

(26) Parr, R. G.; Chattaraj, P. K. *J. Am. Chem. Soc.* **1991**, *113*, 1854.

(27) For a formal proof, it is assumed that the chemical potential and the temperature are constant.

(28) Bader, R. F. W. *Can. J. Chem.* **1962**, *40*, 1164.

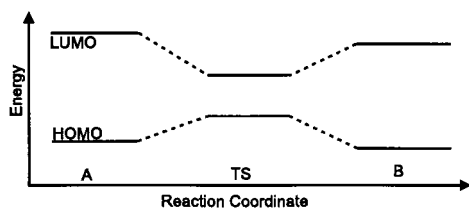


**Figure 1.** Schematic energy level diagram of a class of chemical reactions in which the smallest gap occurs near the transition state (TS).

and a stabilization of the latter and thus a lowering of the gap. Additionally, using a finite difference and frozen orbital approximation, the hardness  $\eta$  of a system can be approximated as  $2\eta \approx \epsilon_{\text{LUMO}} - \epsilon_{\text{HOMO}}$ ,<sup>23</sup> if the system is softer near the activation barrier, then the gap near the transition state will be smaller than the one at the equilibrium structure. An enhanced sampling of activated structures, and hence an increased reactivity, can therefore be obtained by employing a bias potential that lowers the energy for all configurations with a small gap. A straightforward way of obtaining such a bias potential is a simulation with a finite electronic temperature.

DFT was generalized to finite electronic temperatures by Mermin<sup>29</sup> using a free energy functional. A simple form is given by<sup>31</sup>

$$F[\{R_i\}, T^e] = \min_{\{\psi_i\}, \{f_{ij}\}} \int f_{ji} \psi_i^* (\hat{T} + \hat{V}_{\text{ext}}) \psi_j \, dr + E_{\text{Hxc}}[n, T^e] - T^e S[\{f_{ij}\}] \quad (1)$$

Here  $\{\psi_i\}$  are the orthonormal Kohn–Sham wave functions,  $n$  is the electron density,  $T^e$  is the electronic temperature,  $f$  is the occupation matrix,  $\hat{T}$  is the kinetic energy operator,  $\hat{V}_{\text{ext}}$  is the external potential,  $E_{\text{Hxc}}$  is the Hartree and the exchange and correlation functional, and  $S$  is the entropy term given by  $-tr(f \ln(f) + (1-f) \ln(1-f))$ . The solution of eq 1 implies an iterative, self-consistent computation of wave functions and occupation numbers. The latter are calculated using the Fermi–Dirac distribution, that is,  $f_i = 1/(e^{\beta(\epsilon_i - \mu)} + 1)$ , where  $\epsilon_i$  is the eigenvalue of the wave function  $\psi_i$ , and  $\mu$  is the chemical potential, which is determined by the number of electrons in the system. The free energy can be used as a potential energy surface for the dynamics of the ions, and recent advances in computational methodology made it possible to use the free energy functional for first-principles MD.<sup>31–33</sup> We remark that due to the entropy part of the free energy functional, the free energy of a system at a finite temperature is always lower than its (free) energy at zero temperature. However, only if the occupation numbers are significantly different from zero and one (respectively two for spin restricted calculations), the entropy term is nonzero. Hence, for a fixed electronic temperature, the free energy will be more strongly lowered for a system with a small gap than for systems with a large gap. We can thus consider the difference between the finite temperature (FT) potential ( $V_{\text{FT}}$ ) and the zero temperature (ZT) potential ( $V_{\text{ZT}}$ ) as a bias potential ( $V_{\text{bias}} = V_{\text{FT}} - V_{\text{ZT}}$ ) that enhances, often by

many orders of magnitude, the exploration of regions with small electronic gaps. All thermodynamic averages, including free energies and rate constants within the transition state theory approximation,<sup>34</sup> can be obtained exactly from a simulation on the FT potential energy surface, since the following equation relates the thermodynamic average of a function  $f$  in the biased with the one in the unbiased system:<sup>30</sup>

$$\langle f(p, q) \rangle_{\beta\text{H}} = \langle f(p, q) e^{\beta H' - \beta H} \rangle_{\beta\text{H}'} \frac{1}{\langle e^{\beta H' - \beta H} \rangle_{\beta\text{H}'}} \quad (2)$$

where  $\beta$  and  $H$  refer to the original ensemble and  $H' = H + V_{\text{bias}}$  to the biased system. This requires an additional electronic structure calculation at every configuration to compute the ZT energy, which can normally be done with small additional cost since the FT wave functions are a very good initial guess for the self-consistent minimization at ZT. Note that the electronic temperature can be chosen independently of the ionic temperature. For the systems considered here, the temperature of the electrons will typically be a few thousand degrees, whereas the ions are at room temperature.

Within a frozen orbital approximation and at low temperatures (i.e., only the HOMO and LUMO are fractionally occupied), the force on the ions due to the bias potential is given by:

$$\frac{\partial V_{\text{bias}}}{\partial R} \propto \int dr \sum_{\text{HOMO, LUMO}} \frac{\partial}{\partial R} \frac{\delta f_i \psi_i^* \psi_i}{|r - R|} \quad (3)$$

This force is largest on the atoms where the HOMO and LUMO have a nonnegligible magnitude. From a sampling point of view, this is a clear advantage since only the chemically reactive part, and not the remainder of the system, is affected. We note that the driving force is an approximation to the sum of the nuclear Fukui functions ( $\Phi = (\partial F / \partial N)_v$ , where  $F$  is the force on the nuclei,  $N$  the number of electrons, and  $v$  the external potential) of the system. It can indeed be shown that within a frozen orbital approximation, their sum is proportional to the right-hand side of eq 3.<sup>35</sup>

As for all bias potential techniques, a good choice of the biasing parameters is essential. It is an advantage of FTAA that the extent in which the bias potential lowers the barrier is related to a single bias parameter, namely  $T^e$ . More importantly, a good estimate about the optimal value of  $T^e$  can be made on the basis of the gap of the stable system. To be effective, the temperature should be such that near the transition state the HOMO and LUMO are fractionally occupied. Because the gap near the transition state is generally not known, it is useful to establish an upper limit for  $T^e$  that will still guarantee an efficient sampling. Although barriers are lowered with increasing  $T^e$ , a temperature that is too high will yield a too distorted potential energy surface, and configurations that are not relevant for the ground-state ensemble. As demonstrated in the next section, we found that setting  $T^e$  such that  $f_{\text{LUMO}} \approx 0.05$  at the equilibrium configuration gave a significant lowering of the barriers for almost all systems, leaving the overall positions of the minima unchanged. This value is an empirical estimate and depends on

(29) Mermin, N. D. *Phys. Rev.* **1965**, *137*, A1441.

(30) Chandler, D. *Introduction to Modern Statistical Mechanics*; Oxford University Press: New York, 1987.

(31) Marzari, N.; Vanderbilt, D.; Payne, M. C. *Phys. Rev. Lett.* **1997**, *79*, 1337.

(32) Alavi, A.; Kohanoff, J.; Parrinello, M.; Frenkel, D. *Phys. Rev. Lett.* **1994**, *73*, 2599.

(33) VandeVondele, J.; De Vita, A. *Phys. Rev. B* **1999**, *60*, 13241.

(34) The real rate constant is a dynamical quantity and cannot be obtained from a biased simulation.

(35) De Prof, F.; Shubin, L.; Geerlings, P. *J. Chem. Phys.* **1998**, *108*, 7549.

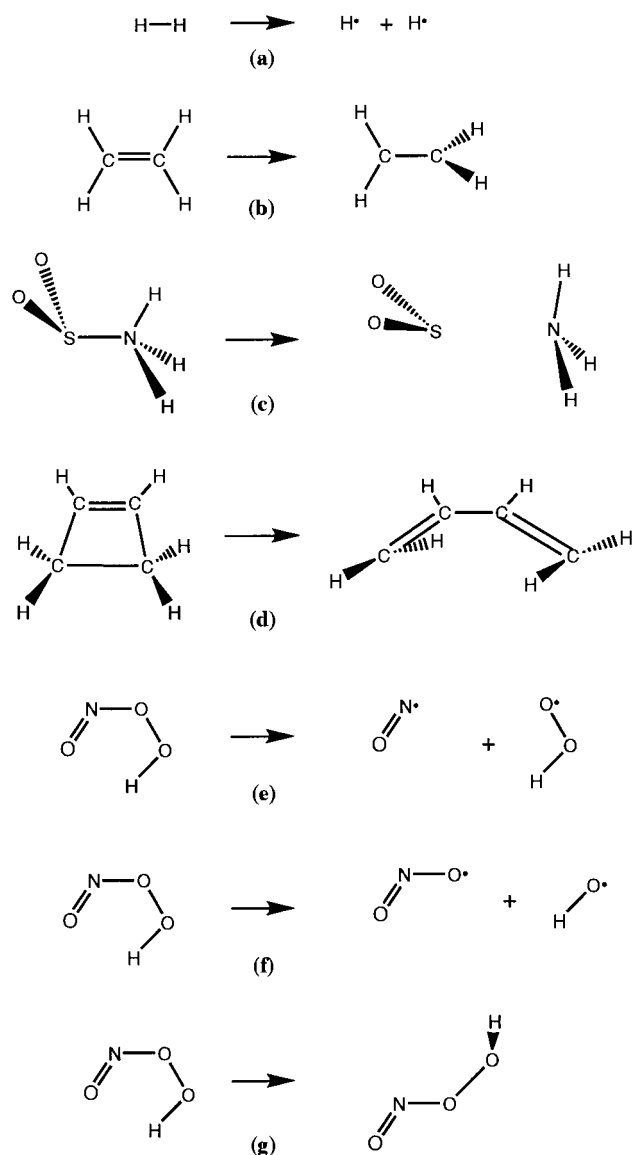


**Figure 2.** The prototypical reactions described in the text: (a)  $\text{H}_2$  dissociation; (b) cis–trans isomerization in  $\text{C}_2\text{H}_4$ ; (c)  $\text{SO}_2$ – $\text{NH}_3$  dissociation; (d) ring opening in cyclobutene; (e) N–O dissociation in peroxyxynitrous acid; (f) O–O dissociation in peroxyxynitrous acid; (g) cis–trans isomerization in peroxyxynitrous acid.

the system under investigation, but provides a useful initial guess for tuning the electronic bias.

### III. Results For Reactions in Gas and in Liquid Phase

To probe the efficiency of a finite electronic temperature in lowering chemical activation barriers, we have applied this approach to a series of prototypical reactions in gas and condensed phase: (III.A.) Homolytic bond dissociation of  $\text{H}_2$  (shown schematically in Figure 2a), (III.B.) cis–trans isomerization of ethene (shown schematically in Figure 2b), (III.C.) Lewis acid–base reaction of sulfur dioxide and ammonia (shown schematically in Figure 2c), (III.D.) conrotatory ring opening of cyclobutene to butadiene (shown schematically in Figure 2d), (III.E.) different reaction channels of peroxyxynitrous acid, (III.E.1.) dissociation of the N–O single bond (shown schematically in Figure 2e), (III.E.2.) dissociation of the peroxy bond (shown schematically in Figure 2f), (III.E.3.–III.E.4.) cis–

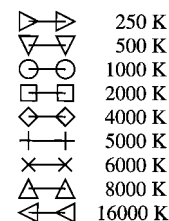


**Figure 3.** Symbols for the electronic temperature used in Figures 4–10.

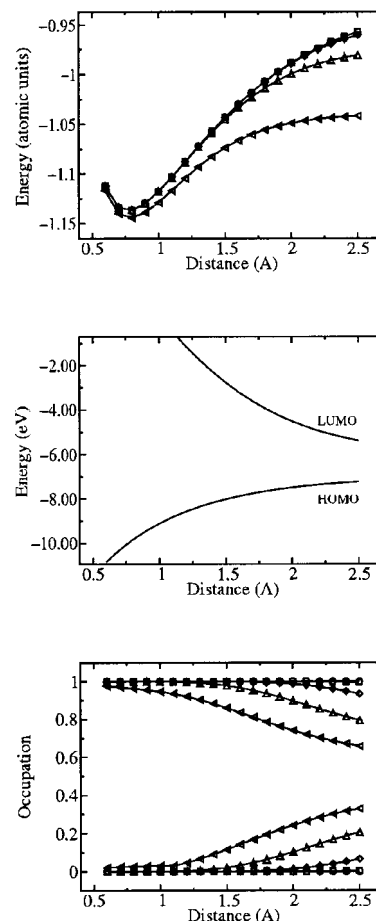


**Figure 4.** Reaction coordinate profiles for the dissociation of  $\text{H}_2$ . The reaction coordinate is the distance between the two hydrogen atoms. The upper panel shows the total energy for several values of the electronic temperature, the middle panel shows the evolution of the eigenvalues of HOMO and LUMO for the zero temperature case, and the lower panel shows the occupation of HOMO and LUMO for several values of the electronic temperature. The different symbols correspond to different electronic temperatures as defined in Figure 3.

trans isomerization around the central N–O bond (in gas phase and in aqueous solution) (shown schematically in Figure 2g).

The main objective of these tests was to establish if a finite electronic temperature can be used to lower significantly chemical activation barriers or, equivalently, to enhance the sampling efficiency without introducing undesirable distortions of the potential energy surface. For the reactions III.A.–III.E., we have therefore examined the energy profiles along appropriately chosen reaction coordinates for different electronic temperatures and compared them with the 0 K results (upper panels of Figures 4–10). In parallel, we monitored the evolution of the eigenvalues (middle panels of Figures 4–10) and the occupation of the Kohn–Sham one-particle states (lower panels of Figures 4–10) along the reaction path. We would like to



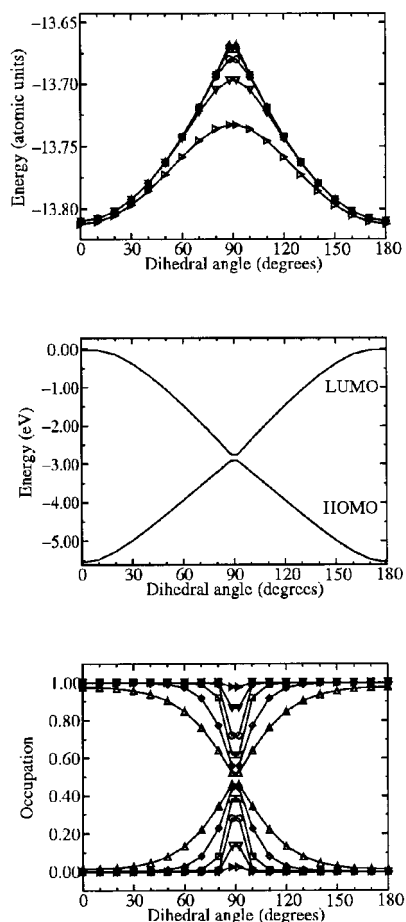


**Figure 5.** Reaction coordinate profiles for the cis–trans isomerization of  $C_2H_4$  as a function of the dihedral angle H–C–C–H. The data are organized and labeled as in Figure 4.

stress that we have chosen to follow predefined reaction pathways for these simple prototypical reactions to facilitate a comparison of the potential energy surfaces at different  $T^e$ . Such a priori information, however, is not mandatory for general applications of FTAA which is designed to accelerate rare reactive events without any knowledge about possible atomic reaction coordinates.

The energy profiles shown in Figures 4–10 allow an inspection of the distortions of the potential energy surfaces at different temperatures. Preserving the essential features of the potential energy surface is important for all biasing schemes, even though eq 2 guarantees that biased sampling gives exact results in all cases. However, the sampling effort increases if new minima configurations or additional channels appear on the biased potential energy surface. In that case, the sampling probes regions of phase space that are not representative for the original ground-state ensemble. For the reactions in sections III.A.–III.D., it can be inferred from the energy profiles, calculated at various electronic temperatures using the optimized zero temperature structures, that the locations of the minima and transition states are basically unchanged. A more elaborate test was performed for the systems in section III.E., for which the geometry along the reaction coordinate was reoptimized for every electronic temperature. It was observed that the deviations of the geometry were small throughout. In particular, the root-mean-square deviation (RMSD) between the low- and high-temperature (5000 K) structures of both the stable cis and the

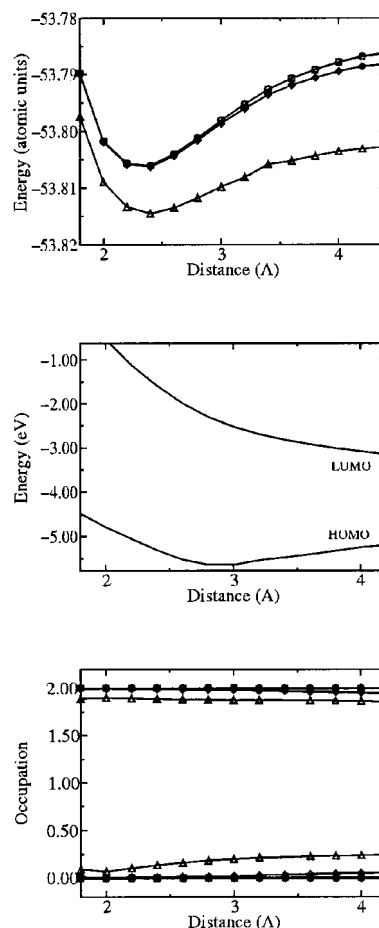


**Figure 6.** Reaction coordinate profiles for the dissociation of  $SO_2-NH_3$  with the distance between the S and N atoms as reaction coordinate. The data are organized and labeled as in Figure 4.

stable trans configurations was less than  $0.02 \text{ \AA}/\text{atom}$ . The maximum RMSD ( $0.07 \text{ \AA}/\text{atom}$ ) was observed at the transition state for cis–trans isomerization, mainly caused by an elongation of 10% of the N–O bond. This small change, combined with the fact that the finite temperature bias potential accelerates the cis–trans isomerization by 5 orders of magnitude (vide infra), guarantees that the sampling of the modified surface and the averaging using eq 2 can be performed with high efficiency.

All of the calculations were performed with the first-principles molecular dynamics program CPMD,<sup>36</sup> using finite temperature DFT<sup>29</sup> in the implementation of Alavi et al.<sup>32</sup> in the framework of pseudo potential theory, periodic boundary conditions, and a plane wave basis set.

**III.A. Homolytic Bond Dissociation of  $H_2$ .** As discussed in the previous section,  $H_2$  can be considered as a prototypical two-level (HOMO–LUMO) system with one bonding and the corresponding antibonding molecular orbital. The equilibrium structure has a large gap that gradually disappears when approaching the dissociation limit. As a consequence, even relatively high electronic temperatures leave the equilibrium occupation almost unaffected, whereas at the same temperature the dissociated state is distinctly stabilized by a significant population of the virtual orbital. Therefore, this system consti-

(36) CPMD Hutter, J.; Alavi, A.; Deutsch, T.; Bernasconi, M.; Goedecker, S.; Marx, D.; Tuckerman, M.; Parrinello, M. MPI für Festkörperforschung and IBM Zurich Research Laboratory, 1995–1999.

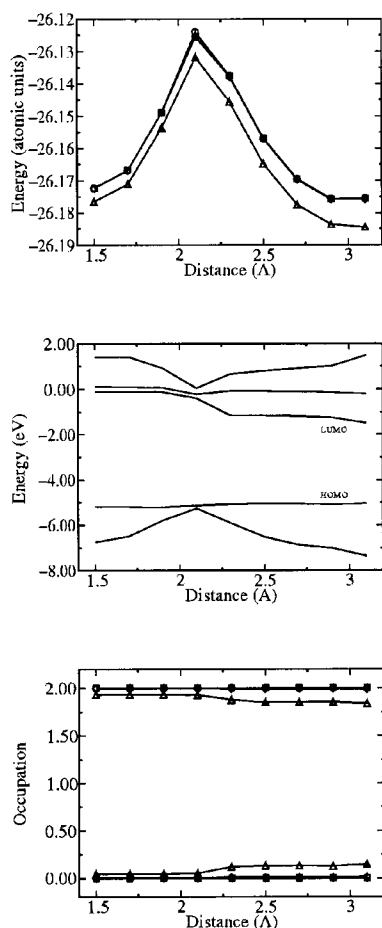


**Figure 7.** Reaction coordinate profiles for ring opening in cyclobutene, where the distance between the two terminal C atoms is the reaction coordinate. The data are organized and labeled as in Figure 4.

tutes a model reaction for which the enhanced sampling approach presented here can be expected to work ideally. The total energy, the eigenvalue spectrum, and the occupations during the dissociation process are shown in Figure 4 for different electronic temperatures. Because of the large gap in the ground-state structure, we can use temperatures up to 16 000 K without inducing any significant changes in the equilibrium geometry. As shown in Table 1, the dissociation energy, on the other hand, is greatly reduced at finite electronic temperature, for example, by ca. 50 kcal/mol at 16 000 K, leading to a drastic enhancement of sampling efficiency by a factor of  $10^{42}$  at room temperature.

**III.B. Rotation around the C–C Bond in  $C_2H_4$ .** The rotational barrier around the C–C bond in ethene requires an activation energy of 88 kcal/mol at the BLYP level of theory. The cis–trans isomerization of ethene is thus an example of a reactive rare event that is clearly beyond the time scale accessible to first-principles molecular dynamics simulations. Considering only  $\pi$ -electrons, also this system can be regarded as another example of a typical two-level (HOMO–LUMO) system, in this case involving  $\pi$  and  $\pi^*$  molecular orbitals. Similar to the situation encountered for the dissociation of  $H_2$ , these two orbitals become degenerate at the top of the rotational barrier at an H–C–C–H dihedral angle of  $90^\circ$ ; that is, also this system has a finite gap at equilibrium which vanishes at the transition state. Hence, the introduction of a finite electronic temperature has a pronounced effect on the rotational barrier

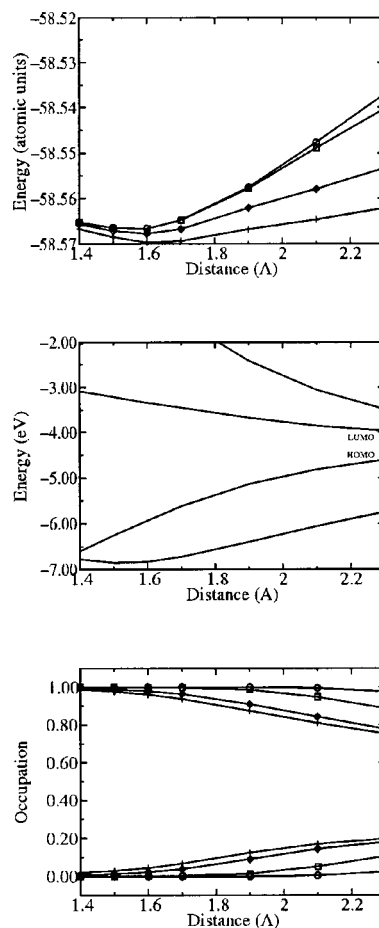


**Figure 8.** Reaction coordinate profiles for N–O bond breaking in ONOOH where the distance between the N and O atoms is the reaction coordinate. The data are organized and labeled as in Figure 4.

(Figure 5 and Table 2), while the location of the stationary points remains essentially untouched. Even at an electronic temperature of 8000 K, the population of the one-particle Kohn–Sham orbitals of the equilibrium structure is close to the 0 K values. At the transition state, on the other hand, HOMO and LUMO are equally populated, and the rotational barrier is reduced by 39 kcal/mol. This lowering of the activation barrier for cis–trans isomerization corresponds to an impressive enhancement of the reaction rate at room temperature by roughly 34 orders of magnitude.

**III.C. Dissociation of the Lewis Acid–Base Complex of Sulfur dioxide and Ammonia.** The reaction of  $SO_2$  and  $NH_3$  is a typical example of a Lewis acid–base reaction, where the electron pair of the  $NH_3$  group is donated to the acceptor  $SO_2$ . One can, therefore, expect that also this reaction is largely HOMO–LUMO dominated. As the reaction is barrierless in gas phase, we monitor here the effect on the reverse reaction, that is, the dissociation of the Lewis acid–base complex. As in the previous examples, a considerable lowering of the dissociation barrier can be observed upon increasing the electronic temperature (Figure 6 and Table 3). At an electronic temperature of 8000 K, it is basically halved. Again the HOMO–LUMO gap is reduced near the dissociation limit with respect to the value at equilibrium (Figure 6, middle panel) leading to a preferential lowering of the dissociated state, while for all of the electronic temperatures used the equilibrium distance itself

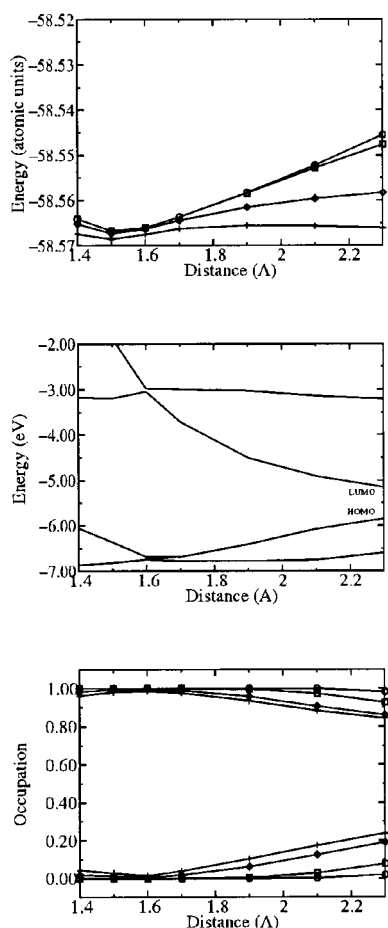


**Figure 9.** Reaction coordinate profiles for O–O bond breaking in ONOOH where the distance between the O atoms is the reaction coordinate. The data are organized and labeled as in Figure 4.

remains unaffected; that is, the overall topology of the potential energy surface is maintained.

**III.D. Conrotatory Ring Opening in Cyclobutene.** The ring opening of cyclobutene to butadiene, one of the classic examples of a symmetry-controlled reaction, is one of the processes of more complex nature that we have investigated here. We have followed the symmetry-allowed, conrotatory pathway as the lowest energy reaction channel by choosing the distance of the two terminal carbon atoms as reaction coordinate. The orbital picture for the symmetry-allowed conrotatory ring opening differs distinctly from the one of the symmetry-forbidden, disrotatory reaction. Whereas for the latter the reactive properties are dominated by the HOMO energy, this is not the case for the former. In the conrotatory case, the HOMO energy is rather insensitive to changes in the reaction coordinate, but a lower lying state, the HOMO-1, can instead be considered as the effective frontier orbital (Figure 7, middle panel). As can be seen in Figure 7, also the LUMO energy shows relatively little correlation with the reaction coordinate, resulting in a situation in which the gap is lowest for the butadiene product. As expected, no dramatic lowering of the activation barrier is observed when a finite electronic temperature is introduced. We note that the occupation numbers are assigned using the Fermi–Dirac distribution, and hence the finite temperature mainly affects HOMO and LUMO. However, due to the fact that also the occupation of the HOMO – 1, LUMO + 1, and LUMO + 2 is influenced by the finite temperature bias, though to a lesser

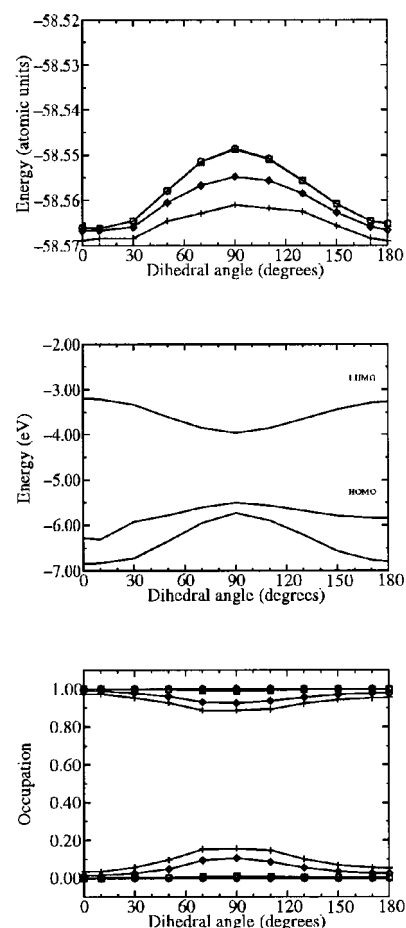


**Figure 10.** Cis–trans isomerization in ONOOH where the dihedral angle O–N–O–O is the reaction coordinate. The data are organized and labeled as in Figure 4.

**Table 1.** Homolytic Bond Dissociation of H<sub>2</sub> at Different Electronic Temperatures<sup>a</sup>

temperature (K)	$\Delta E$ (kcal/mol)	enhancement
1000	0	1
2000	0	1
4000	2	70
8000	15	$6 \times 10^{12}$
16 000	48	$1 \times 10^{42}$

<sup>a</sup>  $\Delta E$  is the lowering of the dissociation energy in kcal/mol, and enhancement is an estimate of the corresponding increase in sampling efficiency for a simulation at room temperature, or, equivalently, the increase in the rate constant at room temperature ( $\sim \exp(\Delta E/kT)$ ).

**Table 2.** Cis–Trans Isomerization of Ethene at Different Electronic Temperatures<sup>a</sup>

temperature (K)	$\Delta E$ (kcal/mol)	enhancement
250	0	1
500	0	2
1000	2	100
2000	7	$2 \times 10^6$
4000	18	$5 \times 10^{15}$
8000	39	$6 \times 10^{33}$

<sup>a</sup>  $\Delta E$  is the lowering of the activation barrier for cis–trans isomerization, enhancement is an estimate of the corresponding increase in sampling efficiency for a simulation at room temperature, or, equivalently, the increase in the rate constant at room temperature ( $\sim \exp(\Delta E/kT)$ ).

extent than the HOMO and LUMO themselves, a small reduction of the barrier can be detected (Table 4), but the overall finite temperature behavior is more complex.

**Table 3.** Dissociation of the Complex  $\text{SO}_2\text{-NH}_3$  for Different Electronic Temperatures<sup>a</sup>

temperature (K)	$\Delta E$ (kcal/mol)	enhancement
1000	0	1
2000	0	1
4000	1	9
8000	5	$3 \times 10^4$

<sup>a</sup>  $\Delta E$  is the lowering of the dissociation energy in kcal/mol, enhancement is an estimate of the corresponding increase in sampling efficiency for a simulation at room temperature, or, equivalently, the increase in the rate constant at room temperature ( $\sim \exp(\Delta E/kT)$ ).

**Table 4.** Conrotatory Ring Opening of Cyclobutene<sup>a</sup>

temperature (K)	$\Delta E_1$ (kcal/mol)	enhancement <sub>1</sub>	$\Delta E_2$ (kcal/mol)	enhancement <sub>2</sub>
1000	0	1	0	1
2000	1	6	1	6
4000	1	6	1	5
8000	2	90	-1	0.3

<sup>a</sup>  $\Delta E_1$  and  $\Delta E_2$  are the lowering of the barrier for ring opening and ring closing, respectively. The corresponding enhancements<sub>1,2</sub> are an estimate of the change in rate constant for the reactions at room temperature.

**Table 5.** N–O Bond Dissociation in ONOOH<sup>a</sup>

temperature (K)	$\Delta E$ (kcal/mol)	enhancement
1000	0	1
2000	2	50
4000	9	$2 \times 10^8$
5000	14	$9 \times 10^{11}$

<sup>a</sup>  $\Delta E$  is the lowering of the dissociation energy in kcal/mol, enhancement is an estimate of the corresponding increase in sampling efficiency for a simulation at room temperature, or, equivalently, the increase in the rate constant at room temperature ( $\sim \exp(\Delta E/kT)$ ).

**III.E. Peroxynitrous Acid.** Peroxynitrous acid is an example of a small molecule for which different reactive pathways with competitive barriers exist. It constitutes, therefore, an interesting test system to probe the relative efficiency of an enhanced sampling method for multiple reaction channels.

Starting from the global minimum configuration (the cis–cis isomer), the molecule can undergo homolytic bond breakage of either the central N–O bond or the O–O peroxy bond and dissociate into N–O• and •O–O–H, or O–N–O• and •O–H, respectively. In addition, the molecule can also isomerize around the central N–O bond to a trans–perp form. We have determined the gas-phase energy profiles at different electronic temperatures for all three reactions. As an important test of our method, we have also investigated the corresponding effects for the isomerization reaction in an explicit solvent.

**III.E.1. N–O Bond Cleavage.** The first reaction channel we studied was the N–O bond cleavage of peroxynitrous acid in which the NO• and •OOH radicals are produced. As can be seen in Figure 8 (middle panel), this reaction has a strong HOMO–LUMO dependence, and, accordingly, the method is able to lower the barrier significantly (Table 5). At the same time, the equilibrium geometry is basically unchanged (RMSD of 0.014 Å/atom) with respect to the 0 K results. At the highest electronic temperature, only a small barrier for dissociation remains, and we verified that during a molecular dynamics simulation the system is able to overcome the barrier and dissociate spontaneously on a subpicosecond time scale.

**III.E.2. O–O Bond Cleavage.** A further reaction that can take place in this system is the breakage of the peroxy bond

**Table 6.** O–O Bond Dissociation in ONOOH<sup>a</sup>

temperature (K)	$\Delta E$ (kcal/mol)	enhancement
1000	0	1
2000	1	10
4000	8	$5 \times 10^6$
5000	11	$8 \times 10^9$

<sup>a</sup>  $\Delta E$  is the lowering of the dissociation energy in kcal/mol, enhancement is an estimate of the corresponding increase in sampling efficiency for a simulation at room temperature, or, equivalently, the increase in the rate constant at room temperature ( $\sim \exp(\Delta E/kT)$ ).

**Table 7.** Cis–Trans Isomerization of Peroxynitrous Acid in Gas Phase<sup>a</sup>

temperature (K)	$\Delta E_1$ (kcal/mol)	enhancement <sub>1</sub>	$\Delta E_2$ (kcal/mol)	enhancement <sub>2</sub>
1000	0	1	0	1
2000	0	1	0	1
4000	4	$1 \times 10^3$	3	400
5000	6	$2 \times 10^5$	5	$5 \times 10^4$

<sup>a</sup>  $\Delta E_1$  and  $\Delta E_2$  are the lowering of the barrier for the rotation from cis to trans and from trans to cis, respectively. The corresponding enhancements<sub>1,2</sub> are an estimate of the change in rate constant for the reactions at room temperature.

with the result of forming •OH and •ONO radicals. This dissociation shows an almost equally strong HOMO–LUMO dependence (Figure 9, middle panel). Accordingly, also for this channel the activation energy is lowered drastically upon introduction of a finite electronic temperature (Table 6), and the rate is enhanced by as much as 9 orders of magnitude.

**III.E.3. Cis–Trans Isomerization.** As for the homolytic bond breakage reactions, we find a strong dependence on the electronic temperature also in the case of the cis–trans isomerization of peroxynitrous acid (Table 7). The characteristic evolution of the gap along the reaction coordinate (i.e., the ONOO dihedral angle), shown in Figure 10, renders this system an almost ideal case for FTAA. Indeed, FTAA leads to a maximal lowering of 6 kcal/mol at  $T^e = 5000$  K and therefore to an acceleration factor of approximately  $10^5$  at room temperature. Moreover, this study on peroxynitrous acid also illustrates the power of FTAA in the sense that three different competitive chemical reactions can be easily accelerated significantly by a single and straightforward electronic bias. This is in contrast to a typical geometrical bias that forces the system in a priori selected direction.

**III.E.4. Cis–Trans Isomerization in Solution.** The acceleration of chemical events in complex systems with a rugged potential energy landscape in which the barriers of the effective chemical events coexist with a multitude of low conformational barriers is especially challenging. Most of the existing methods lack the ability of finding relevant high lying activation barriers in a sea of less important transition states. A method that is able to enhance the sampling in a selective way for the chemical event only is, therefore, highly desirable. The cis–trans isomerization of peroxynitrous acid in an explicit solvent of 52 water molecules at normal density, both treated at the gradient-corrected DFT level, thus constitutes a challenging test, to probe if the method presented here is able to lower selectively chemically relevant reactions in the presence of many chemically less relevant nearby transition states. Because the calculation of a complete free energy profile for this reaction is computationally very demanding, we decided to study the influence of the electronic temperature for selected configurations only.



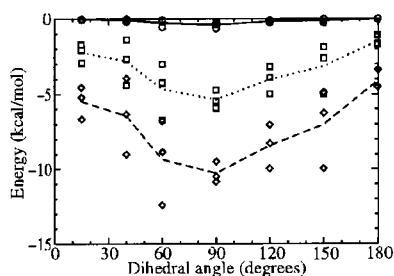


**Figure 11.** The lowering of the total energy as compared to the value at zero temperature, for selected configurations of peroxynitrous acid in solution during the cis–trans isomerization. Different symbols represent values obtained for different electronic temperatures: ○, 2000 K; □, 4000 K; ◇, 5000 K. The lines are drawn through the average values for the respective temperatures.

These configurations were obtained from a previous first-principles molecular dynamics study<sup>37</sup> that used constrained MD to calculate the free energy profile for isomerization in aqueous solution. We used three independent configurations for several values of the reaction coordinate to calculate the average lowering of the total energy as a function of the electronic temperature. Clearly, this does not provide sufficient statistics to obtain quantitatively converged results but can give a first qualitative indication on the performance of the enhanced sampling approach for a reaction in condensed phase. As shown in Figure 11, the fluctuations in the observed barrier lowering are quite significant indicating the strong dynamical solvent effect on the gap of the system. Notwithstanding, the introduction of a finite electronic temperature leads to a significant lowering of the activation barrier (Table 8). Note that the achieved enhancement in sampling efficiency is comparable to the values obtained for the corresponding gas-phase reaction. These results indicate that the finite temperature approach can be equally effective for gas-phase as well as for condensed-phase systems.

#### IV. Conclusions

We have presented a novel method (finite temperature-assisted acceleration, FTAA) to enhance the sampling of rare

**Table 8.** Cis–Trans Isomerization of Peroxynitrous Acid in Aqueous Solution<sup>a</sup>

temperature (K)	$\Delta E$ (kcal/mol)	enhancement
1000	0	1
2000	0	2
4000	4	$2 \times 10^3$
5000	6	$2 \times 10^5$

<sup>a</sup>  $\Delta E$  is the lowering in activation energy in kcal/mol for conversion from the cis to the trans form, enhancement is an estimate of the corresponding increase in sampling efficiency for a simulation at room temperature, or, equivalently, the increase in the rate constant at room temperature ( $\sim \exp(\Delta E/kT)$ ).

chemical events. Our approach makes direct use of the intrinsic electronic structure of the reactive system by exploiting the simple concept of a finite electronic temperature. By applying FTAA, it is possible to lower the barriers for a number of typical chemical reactions significantly. At the same time, the overall topology of the potential energy surface is maintained, so that the difference between the zero temperature and the finite temperature potential can be used efficiently as a bias potential. Moreover, a similar reduction of activation barriers can also be achieved for solution reactions for which the barrier of the actual chemical event is competing with a large number of energetically low-lying barriers for configurational transitions. The simple method presented here works surprisingly well in the case of orbital-driven chemical reactions that are dominated by the HOMO and LUMO orbitals for which impressive acceleration factors of several orders of magnitude, often more than five, can be achieved in a straightforward manner. FTAA should be considered as a first step toward more advanced electronic bias methods that make direct use of the chemical information inherent in the electronic structure. Advantages of the current scheme are its easy implementation, and for many electronic structure codes, its low computational cost.

**Acknowledgment.** One of the authors (J.V.) acknowledges funding from an ETH internal grant.

JA0126733

(37) Doclo, K.; Rothlisberger, U. *J. Phys. Chem. A* **2000**, *104*, 6464.